공학석사학위논문

스키 진동과 마찰력 사이의 상관관계 해석

A numerical study on the effect of ski vibration on friction

2017년 2월

서울대학교 대학원

기계항공공학부

남 윤 형

스키 진동과 마찰력 사이의 상관관계 해석

A numerical study on the effect of ski vibration on friction

지도교수 김 도 년

이 논문을 공학석사 학위논문으로 제출함

2017년 2월

서울대학교 대학원

기계항공공학부

남 윤 형

남윤형의 공학석사 학위논문을 인준함

2017년 2월

위 원 장 _____

부위원장 _____

위 원 _____

Abstract

Friction in icy condition is a complicate phenomenon usually consisting of three representative regimes: boundary, mixed and hydrodynamic regime. [10] Various factors may affect the friction in these regimes including the thickness of water film, the amount of frictional heat, velocity and apparent contact area. In ski jump, ski plates vibrate when gliding on an icy slop, which may have an influence on the gliding performance as they can alter these factors related to friction.

Here, we present our effort to investigate the effect of vibration on friction numerically using a combined friction model applied to a jump ski. A pressure-dependent friction model is first derived from experimental data measured in small test specimen, which is well agreed with a theoretical model. Then, we construct a numerical, finite element model for a jumping ski such that it shows the same flexural stiffness as characterized experimentally. Finally, we explore how vibration affects the friction by performing simulations with various amplitudes and frequencies of vibration applied.

Keywords : Friction, vibration, Friction model, Jump ski, Finite element model, flexural stiffness

Student Number : 2014-22482

Table of Contents

List of Figures

List of Tables

Nomenclature

Symbols

E	Elastic modulus
I_X	Second moment of area
EI_X	Bending rigidity
P	Force
L_e	Element length
δ	Deflection due to bending
b	Width of element
h	Thickness of element
A	Highest start place of in-run track
B	Lowest start place of in-run track
T	Edge of the takeoff table
e_1	Distance of in-run track from A to T
e_2	Distance of in-run track from B to T
γ	In-run inclination
v	Velocity at time t
v_0	Initial velocity
v_t	Terminal velocity
a	Constant acceleration
s	Distance at time t
s_0	Initial position

t	Time
μ	Friction coefficient in icy condition
μ_l	Friction coefficient for contact length
μ_{dry}	Friction coefficient in dry condition
α	Fraction of unlubricated area
η	Viscosity of water layer
v_l	Relative velocity
h_w	Thickness of water layer
P_r	Pressure
T_{air}	Ambient temperature
A_c	Contact area
L_c	Contact length
F_n	Normal force
w_c	Contact width
w_t	Width of test specimen
F_f	Friction force
g	Gravity
F_0	Vibration amplitude
w	Vibration frequency
M	Mass matrix
C	Damping matrix
K	Stiffness matrix

R	Force vector
U	Displacement vector
$\dot{U}$	Velocity vector
$\ddot{U}$	Acceleration vector
K_{eff}	Effective stiffness matrix
R_{eff}	Effective force vector
ΔU	Displacement increment
Δt	Time interval
i	Number of iteration
R_c	Force vector due to contact and friction
τ	Non-dimensional variable for friction
λ	Normal traction
Φ	Eigenvector
w_n	Natural frequency
λ_n	Eigenvalue

Abbreviations

HS	Hill Sizes of in-run track
FEM	Finite element method
UHMW-PE	Ultra high molecular weight poly ethylene

1. Introduction

The jump ski can consists of four parts; In-run, takeoff, flight and landing and a player who flies further than others gets a good score. There are requirements to improve the performance of each part. The in-run section is the section where the athlete gets the takeoff speed. The faster the final in-run speed before takeoff, the farther he can fly. Thus, low frictional force is important factor. In order to improve the athletes' performance in in-run section, takeoff speed should be increased. To that end, we need to understand the structural characteristics of the jump ski itself and the friction in icy condition. Many previous researches can confirm the phenomenon that the friction force decreases when vibration is applied to an object that performs dynamic behavior.[1, 2, 3, 17, 18]

The preceding researches can be roughly classified into dry friction and ice friction, and briefly introduce the contents. First, the correlation between vibration and friction is analyzed by using coulomb and dahl friction model in dry condition when vibration is applied to a moving object while rubbing: external vibration changes the relative velocity of the object and the average frictional force decrease. [1] In addition, recent study has proposed a modified dahl friction model that reduces the friction coefficient according to the vibration characteristics.[2] On the other hand, an experimental study in icy condition has been conducted in which the frictional force is reduced with vibration as compared to when there is no vibration. [3] However, previous researches have been limited to small and rigid specimens, so research on the relationship between vibration and friction has not carried out when vibrations are applied to objects with structural and geometric characteristics like jump ski. Therefore, when vibration occurs in an object having the structural

characteristics like jump ski, we find out the relationship between vibration and friction through simulation.

In order to simulate the dynamic behavior of the jump ski in in-run section, we first constructed a jump ski model using the finite element to simulate the structure and elastic characteristics of the jump ski composed of long slenderness and composite materials. Next, a friction model in icy condition, which can represent the friction between the in-run track and the base material (UHMW-PE) of jump ski, was derived.

The relationship between external vibration, elasticity of jump ski and friction was analyzed by using our finite element model and induced friction model in icy condition.

2. Method

2.1 Finite element model for jump ski

Jump skis consist of unique shape (long slenderness, camber, etc.) and composite material (wood, rubber, glass fiber, carbon fiber, plastic, etc.). And when the external force is applied to jump ski in a certain direction, jump ski is elastically deformed mainly in thickness direction which means that bending action appears. Thus, the beam element is an appropriate element that can be used to create a finite element model for jump ski.

To construct a finite element model for jump ski, the information on the shape and mechanical properties of actual jump ski is needed. The AJOU UNIVERSITY who is our co-work performs the all experiment and measures geometry and deflection of jump ski by the following method.

The shape data were measured by dividing the actual jump ski into 80 points in total (Figure 1). The bending rigidity of composites material of jump ski was measured by separating the ski into twelve parts based on the important points (Afterbody contact point, Balance point, Forebody contact point and Shovel) and calculated by the deflection equation of cantilever beam on the basis of the deformation measurements of each part. Then, the deflection equation of cantilever beam is

$$EI_X = \frac{PL_e^3}{3\delta} \tag{1}$$

Where P is the applied force and L_e is the length for each section and δ is the deflection of jump ski due to applied force (P) and EI_X is the bending rigidity (Figure 2(C)). In order to realize such a feature as a finite element model,

simulation model was constructed using two dimensional Euler-beam elements based on the shape data of the jump ski obtained through experiments. Next, the elastic modulus of each part for the simulation model of jump ski was obtained by calculating the second moment of area form the cross section on the basis of the bending rigidity (EI_X) data. Then, the equation of second moment of area is

$$I_X = \frac{bh^3}{12} \tag{2}$$

Where b is the width of jump ski and h is the thickness of jump ski (Figure 3).

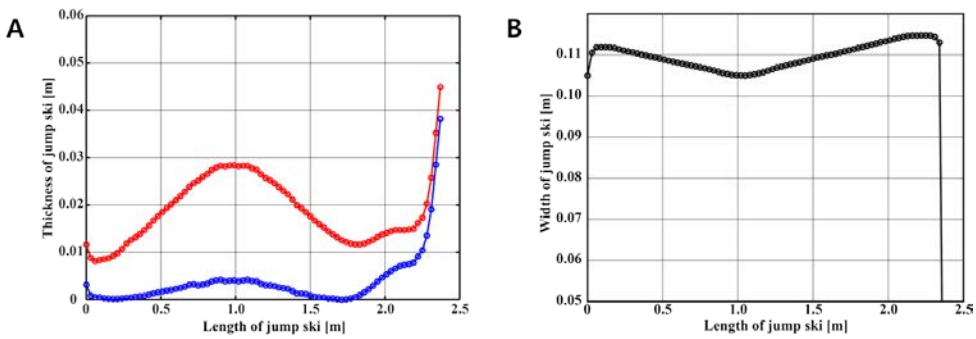

Figure 1. Elan jump ski geometry (Experimental data are proved by Polymer Processing Lab. in AJOU UNIBERSITY), (A) Thickness according to length, (B) Width according to length.

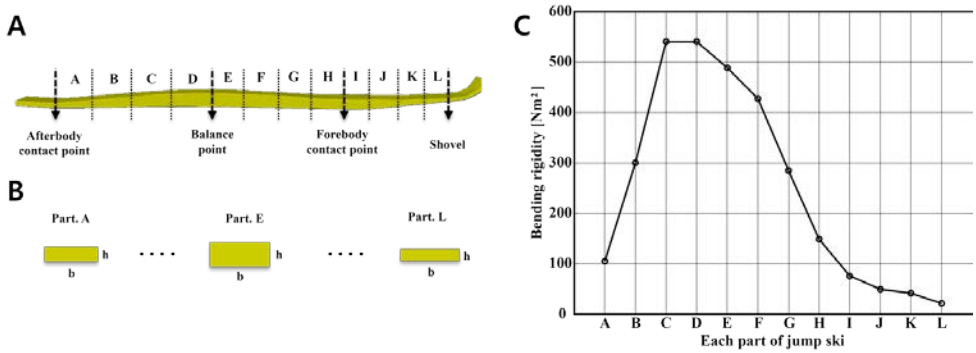

Figure 2. Experimental and geometric data of Elan jump ski (The data are proved by Polymer Processing Lab. in AJOU UNIBERSITY), (A) Important points to separate the jump ski into twelve parts, (B) Cross section area for each part, (C) Bending rigidity for each part.

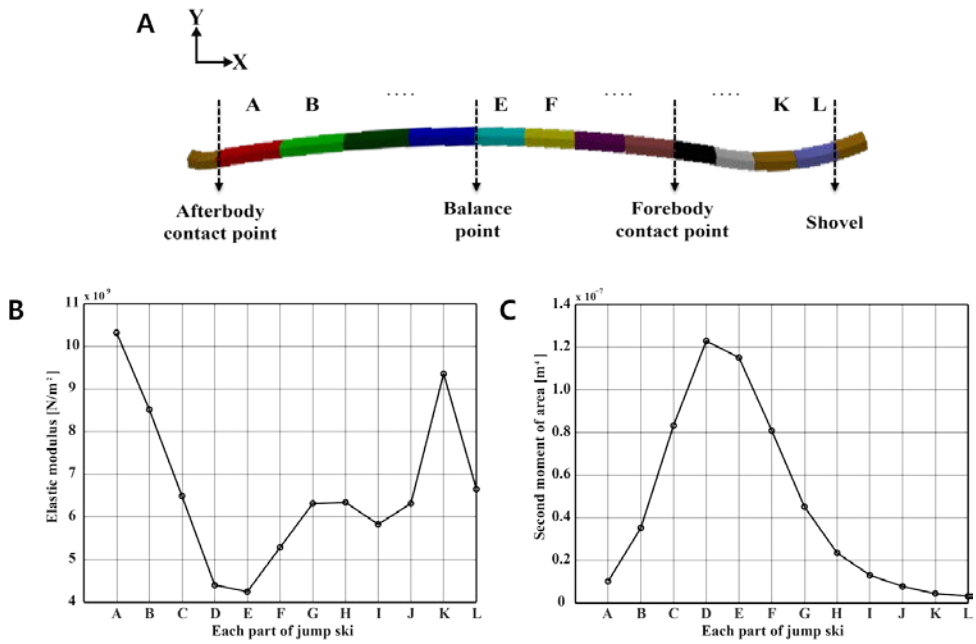

Figure 3. (A) Two dimensional finite element model for Elan jump ski using Euler beam element, (B) Elastic modulus calculated by bending rigidity and second moment of area for each section. (C) Second moment of area for each part calculated from the data of jump ski geometry.

2.2 Definition of skier and ski boots

During the gliding in the in-run track, a skier keeps a certain posture and descends until he takes a leap. In addition, ski boots are relatively hard to bend compared to ski plate. So, both ski boots and skier can be constructed by two-dimensional rigid block using solid element on ski model, each of which is 1.04kg and 31kg (Figure 4).

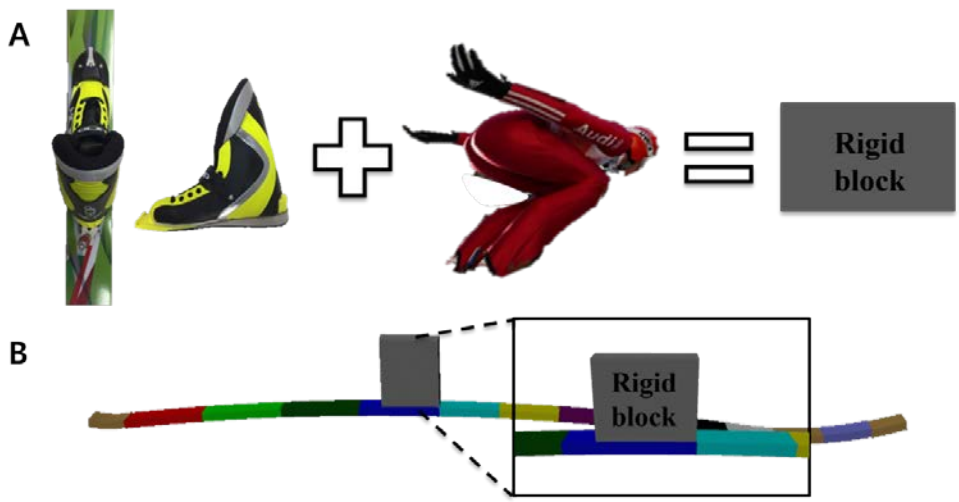

Figure 4. Definition of ski boot and skier, (A) Ski boots is relatively rigid and is fixed on the ski near the balance point and skier keep almost the same posture while playing in in-run section. So, both ski boots and skier can be modeled as a solid block, (B) A finite element model with athlete and boots. The position of the boots is 0.31m behind the balance point.

2.3 Definition of in-run track

Jump skier get a takeoff speed by descending the in-run track with a slop angle by a certain distance from the starting point to the takeoff point. Therefore, it is necessary to have information about the slope angle and the running distance of the actual in-run track so that the motion of the ski can be simulated in the running range.

It can be possible to obtain information about the hill size, terminal velocity right before takeoff and whole time during descent from international competition and to calculate the distance of in-run track and angle of the slope on the basis of standards for the construction of jumping hills. As shown in Figure 5, it can be seen that the hill size is $140m$ (Large hill), the terminal velocity is $26.25m/s$, and whole time is $6\sec$.

The standards for the construction of jumping hills provide information on how to calculate the distance of the in-run track and the angle of slope (Figure 6). The contents are as follows. e_1 and e_2 are the running distance, A is the highest start place, B is lowest start place, HS is hill size, T is takeoff point, γ is the angle of in-run track and the equation of running distance in the in-run track is

$$e_2 = 67.3 - 0.944 \times \gamma + 0.331 \times HS \tag{3}$$

The in-run inclination γ may at most be 37°. In the case of large hill (HS > $90m$), γ should be at least 30°. Using the information on the hill size obtained

from international competition and above equation, it can be possible to calculate the sliding distance according to the in-run inclination γ (Table 1).

The following assumptions, on the other hand, can be made by using the terminal velocity and whole time during descent. First, the in-run track is linear. Second, the initial velocity is zero. Third, the acceleration is constant while jump ski slides down the track. Fourth, there is no air resistance. We calculated the running distance from the Newton's equation of motion with both above assumption and information on running time and terminal velocity. The Newton' equation of motion is

$$v = v_0 + at \tag{4}$$

$$s = s_0 + v_0 t + \frac{1}{2} a t^2 \tag{5}$$

Where v_0 is the initial velocity, v is the velocity at time t, a is constant acceleration during whole time, s_0 is the initial position, s is the distance at time t and t is the time. Both v_0 and s_0 are zero. So, a is equal to $\frac{v}{t} : v_t = 26.25 m/s$, $t = 6\,\text{sec}$ and v_t is equal to $v_t = at$. Thus, the acceleration a is $4.38 m/s^2$ during whole time and the distance of the in-run track is $78.84m$: s is equal to $\frac{1}{2} a t^2$. The angle of in-run track is obtained by comparison between the result calculated from Newton's equation of motion and the result calculated from the equation of running distance in the in-run track. Thus, we can assume that the distance of the in-run track is about $80m$ and the in-run

inclination γ is 36° for the simulation.

Figure 5. Video (http://www.youtube.com/watch?v=MLYnE2TxC7W) about international competition (2011 Winter Asian game), (A) Just before departure. We can obtain the hill size ($140m$), (B) Just before takeoff. We can obtain the terminal velocity ($94.5km/h$) in the in-run track.

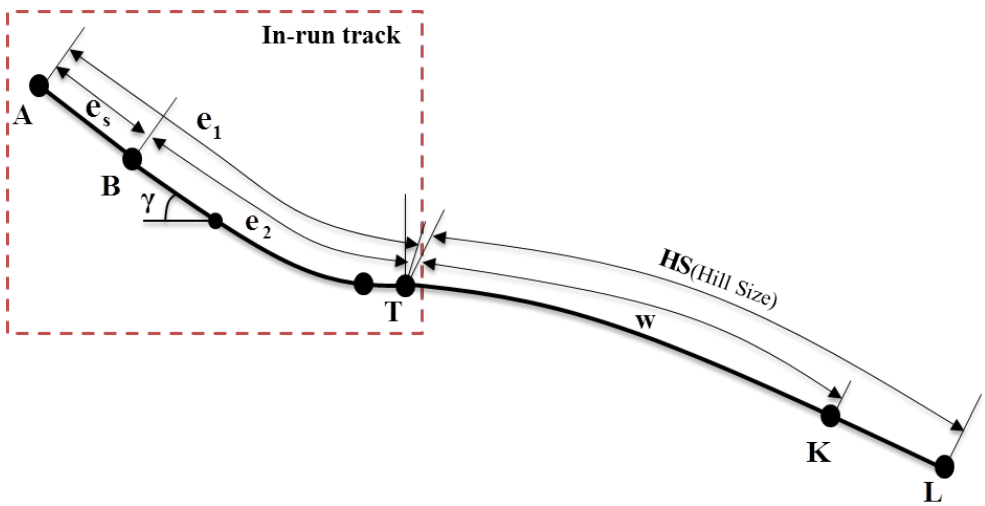

Figure 6. Ski jumping hill (Standards for the Construction of Jumping Hills-2012). A is the highest start place, B is lowest start place, T is edge of the takeoff table, K is construction point, L is the end of the landing area, e_s is the length of start places A until B, e_1 is length of the in-run from A to T, e_2 is length of the in-run from B to T, γ is the gradient of the straight part of the in-run, W is the distance between T and K and HS is the hill size.

In-run inclination [γ]	37°	36°	35°	34°	33°	32°	31°	degree
Distance at time $6\,\mathrm{sec}$	78.71	79.65	80.60	81.54	82.48	83.43	84.37	[m]

Table 1. Distance of in-run track according to angle of slope. The distance at time $6\,\mathrm{sec}$ are calculated by using the equation (3) when the HS (hill size) is $140m$.

2.4 Friction mechanism in icy condition

In order to simulate the jump ski motion in the in-run section, we need to know how to generate the friction between jump ski and ice. Because friction is dominantly influenced by the environment in which the object is situated and is therefore expressed as a function of variables. In particular, the friction mechanism in icy condition occurs through a very complicated process as follows.

At the beginning of friction, ice and objects are subject to dry friction and have a relatively high coefficient of friction. In this case, the heat generated by the friction causes the temperature between the ice and the object to reach the melting point of the ice in about $0.004\,\mathrm{sec}$. Hydrodynamic friction due to generated water layer and dry friction is generated at the same time from this point, and the coefficient of friction is lowered, so that it can be slipped more easily. So, friction in icy condition is divided into three regimes according to the relative relationship between the thickness of the water layer produced by frictional heat and the surface roughness of both ice and object: boundary, mixed and hydrodynamic regime.

There is water layer in the boundary regime. But it is formed very thin, so that the dry friction between the object and the ice is dominant. The mixed regime is the regime where the dry friction between the object and the ice and the thickness of water layer generated by frictional heat coexist harmoniously. Finally, the water layer is thickly formed and the lubricated friction dominates in hydrodynamic regime. Therefore, the theoretical friction formula in icy condition can be expressed as the sum of dry and lubricated friction as follows. [11]

$$\mu = \alpha\mu_{dry} + (1-\alpha)\frac{\eta v_l}{h_w P_r} \tag{6}$$

Where α is the fraction of dry friction and hydrodynamic friction, μ_{dry} is the dry friction coefficient between object and the ice without water layer, v_l is the relative velocity of the object, η is the viscosity of water layer, h_w is the thickness of the water layer and P_r is the pressure. The units are shown in the following Table 2.

Parameters of equation 6	η	v_l	h_w	P_r	μ_{dry}	μ	α
Units	kg/ms	m/s	nm	N/m^2	Non	Non	Non

Table 2. The units of parameters consisting of equation 6. Friction coefficient is non-dimensional parameter, so the units of dry friction part is non-dimension and the units of hydrodynamic friction part is also non-dimension.

2.5 Parameter study for theoretical friction model in icy condition

Bäurle has recently conducted an experimental study on friction in icy condition. Based on his research, we proceeded with the parameter study on the theoretical friction model in icy condition.

First, we explain the experiment performed by Bäurle and then explain how we obtained the parameters of the theoretical friction model from experimental results. Bäurle built a 1.8 meter test equipment for friction in icy condition and experimented with the material used for the bottom surface of actual ski as a test specimen. When the ambient temperature is $-5^{\circ}C$, he obtained the experimental results on the relationship between the macroscopic area of the specimen, the normal force and friction and the relationship between relative velocity and friction. Namely, as the macroscopic contact area increased, the coefficient of friction increased. As the normal force increased, the coefficient of friction decreased with increasing macroscopic contact area. And the friction coefficient doesn't change when the relative velocity of the moving object was changed. [5]

Based on the above two experimental results, we proceeded with the parameter study as follow. From the experimental results, the experimental data on the friction coefficient and macroscopic area for each normal load are extracted. The data of relationship between the friction coefficient and the macroscopic area is converted into data with respect to the relationship between pressure and friction coefficient. Then, it is possible to drive the following equation using the regression

analysis (Figure 7).

$$\mu = 0.0229 + \frac{9684.5}{P_r} \tag{7}$$

Where P_r represents the pressure. Comparing the theoretical friction model in ice with the friction model obtained through the parameter study, the constant part represents the dry friction regime and the variable part by pressure represents the lubricated friction regime.

Since the finite element model for jump ski is constructed using two-dimensional element, the equation 7 can be expressed as follows.

$$\mu = 0.0229 + \frac{9684.5}{F_n} A_c \tag{8}$$

$$\mu = 0.0229 + \frac{9684.5}{F_n} L_c w_c \tag{9}$$

Where F_n is the normal force, A_c is the contact area, L_c is contact length and w_c is contact width. The width w_t (0.005m) of the test specimen is substituted to derive the friction relation for contact length.

$$\mu = 0.0229 + \frac{48.42}{F_n} L_c \tag{10}$$

It is almost impossible to achieve perfect dry condition without generated water layer when both object an ice come in contact. But Bowden et al. obtain a generally accepted value of dry friction coefficient ($\mu_{dry} = 0.3$) with very thin water layer (not exceeding some nm)[6, 29] From the comparison with the dry friction part of the equation 10 obtained the parameter study based on the experimental results, it can

be deduced that the ratio α of dry friction occupied by 7.6% and the ratio of hydrodynamic friction $1-\alpha$ is 92.4%.

In the final friction model obtained from the parameter studies, we can see that most of frictional forces are caused by hydrodynamic friction. In addition, it is assumed that the effect of other variables (velocity, water layer) is independent of friction. The reason for this as follows.

When friction occurs in icy condition, the relationship between the thickness of water layer produced by frictional heat and the roughness of both surfaces can vary from moment to moment. Also, from a microscopic viewpoint, it is not known how the friction area where actual friction occurs is formed. Therefore, when the theoretical formula is applied, it is assumed that the thickness of the water layer is constant during whole time and the contact area is calculated based on the macroscopic viewpoint.

It is proved by Bäurle that relative velocity of the test specimen is independent of friction.[5]

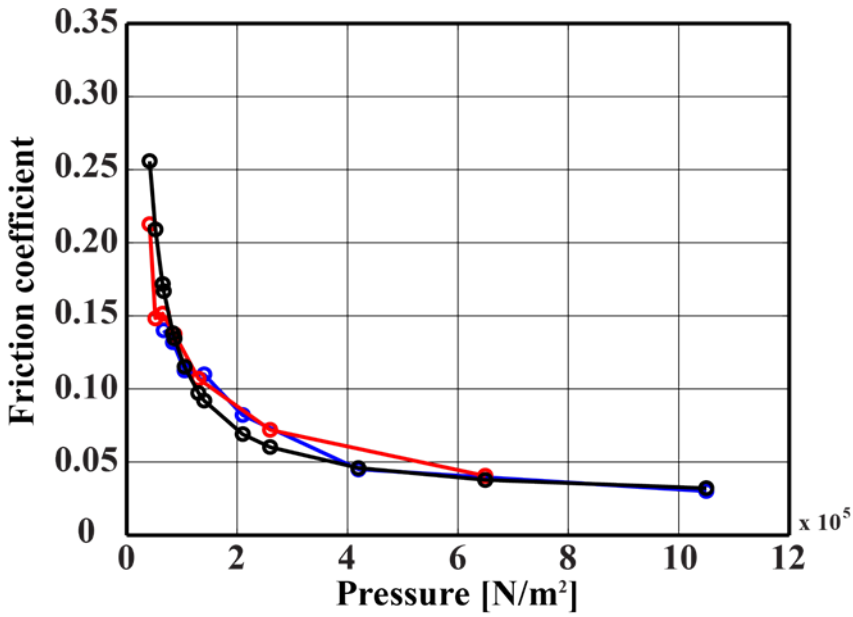

Figure 7. The relationship between pressure and friction coefficient derived from experimental results performed by Bäurle. Blue line represents the relation when normal force is $84N$. Red line represents the relation when normal force is $52N$. Black line represents the result from regression analysis.

2.6 Definition of external vibration

As mentioned in the introduction, there have been many studies to reduce the frictional force when external vibrations are applied to a moving object with friction. Therefore, it can be assumed that friction reduced when vibration is applied to the ski and friction model so far built up. To verify this assumption, we need to know the magnitude of vibration occurring in the actual ski competition.

Akira Shionoya, along with a junior jump skier, measured the vibration that occurs when skiing in a real jump ski arena. Two acceleration sensors were attached to the front and rear of the jump ski to measure the acceleration due to the vibration. A junior jump skier conducted experiments directly at the jump ski arena. The data is gathered in a bag behind him. [9]

Based on his experiments, the maximum magnitude of the acceleration is assumed to be $10m/s^2$. Also since the weight of the ski is $2.5kg$, the maximum amplitude of the vibration for simulation is calculated as $25N$. In the simulation, when the ski model moves with friction, harmonic vibration is applied to both end nodes of the ski model.

3. Results and Discussion

3.1 Static analysis

As described above, we constructed a ski finite element model through experimental results. Therefore, a static analysis was performed to confirm that the elastic characteristics of ski model fit well with the elastic characteristics of the actual jump ski.

Simulation method is the same as the experiment and is as follows. One end of each part was fixed and a constant force of 200N was applied to the opposite end (Figure 8). The amount of deformation was obtained by always setting the fixed part to the side close to the ski binding part. As can be seen in Figure 9, a finite element model for jump ski is constructed in which the simulation results for deflection of each part coincide with the experimental values within 0.5%. And the values of bending rigidity for each part can be calculated by substituting the values of obtained deformation into the δ parameter in equation 1.

Thus, it is possible to simulate the stiffness distribution characteristics of a jump ski composed of composite materials.

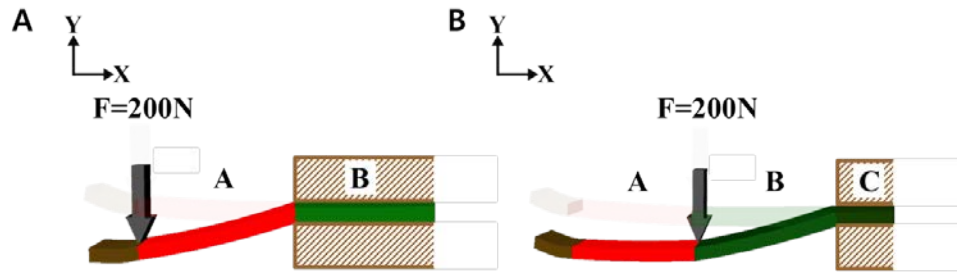

Figure 8. Simulation method for deflection. Constant force $200N$ is applied on the opposite side of the fixed one for each part, (A)Deflection for part A, (B) Deflection for part B.

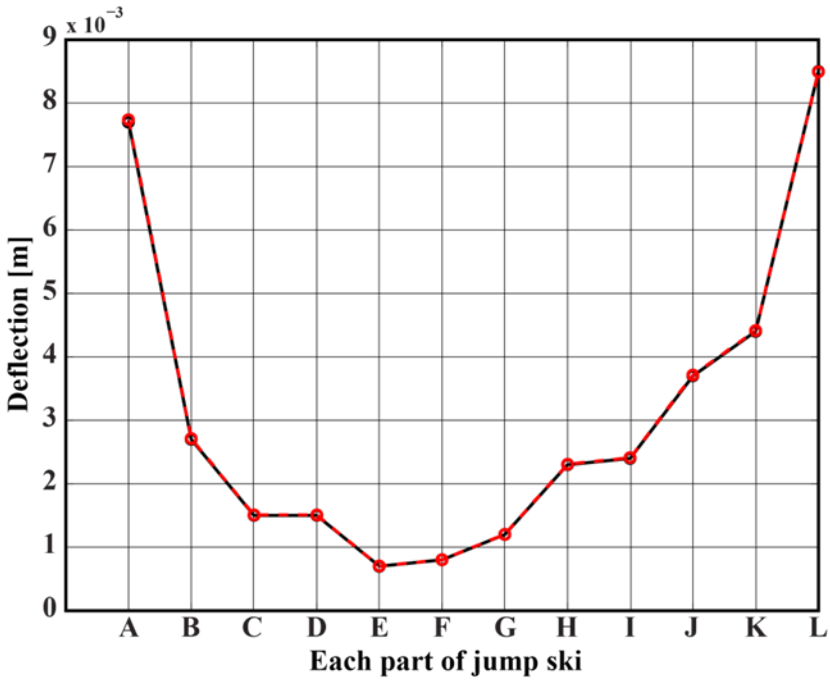

Figure 9. Comparison of deflection for each part between simulation and experiment. The simulation results are very well agreed with experimental results (Error is within 0.5%).

3.2 Dynamic analysis

3.2.1 Time integration method

Generally, the following equilibrium equation is used when simulating a moving object in solid and structural mechanics.

$$M\ddot{U} + C\dot{U} + KU = R \tag{11}$$

Where M is the mass matrix, C is the damping matrix, K is the stiffness matrix, R is the vector of applied force, U is the displacement vector and an overdot is a time derivative.

For the reliable solutions during the entire time of dynamic analysis, we use the composite implicit time integration for nonlinear dynamics.[28] Let's take a brief look at this: t is the current time and all variables is known at time t. The solution which has to be obtained after time interval Δt is divided into two sub-steps.

First, the solution is obtained after time interval $\Delta t / 2$ using the Newmark method (using the trapezoidal rule) as follows.

$$K_{eff} = \frac{16}{\Delta t^2} M + {}^{t+\frac{\Delta t}{2}} K^{(\mathrm{i}-1)} \tag{12}$$

$$R_{eff} = {}^{t+\frac{\Delta t}{2}} R - {}^{t+\frac{\Delta t}{2}} F^{(\mathrm{i}-1)} + M\left(\frac{16}{\Delta t^2}\left({}^{t}\mathrm{U} - {}^{t+\frac{\Delta t}{2}}\mathrm{U}^{(\mathrm{i}-1)}\right) + \frac{8}{\Delta t}\,{}^{t}\dot{\mathrm{U}} + {}^{t}\ddot{U}\right) \tag{13}$$

Where K_{eff} is the effective stiffness matrix, R_{eff} is the effective force vector,

${}^{t+\frac{\Delta t}{2}}K^{(i-1)}$ is the consistent tangent stiffness matrix and F is the vector of nodal forces equivalent to the element stresses. The solution can be found at $t+\frac{\Delta t}{2}$ from two simplified effective matrices.

$$\Delta U^{(i)} = K_{eff}^{-1} R_{eff} \tag{14}$$

$${}^{t+\frac{\Delta t}{2}}U^{(i)} = {}^{t+\frac{\Delta t}{2}}U^{(i-1)} + \Delta U^{(i)} \tag{15}$$

Where $\Delta U^{(i)}$ is the displacement increment at iteration i.

Once the solution to the displacement has been computed at time $t+\frac{\Delta t}{2}$, the acceleration and velocity are calculated by the following relationship

$${}^{t+\frac{\Delta t}{2}}\dot{U} = \frac{4}{\Delta t}({}^{t+\frac{\Delta t}{2}}U - {}^{t}U) - {}^{t}\dot{U} \tag{16}$$

$${}^{t+\frac{\Delta t}{2}}\ddot{U} = \frac{4}{\Delta t}({}^{t+\frac{\Delta t}{2}}\dot{U} - {}^{t}\dot{U}) - {}^{t}\ddot{U} \tag{17}$$

After total solutions of displacement, velocity and acceleration at time $t+\frac{\Delta t}{2}$ are derived from the above procedure, we can calculate the final solution at time t by using three-point backward method.

$$K_{eff} = \frac{9}{\Delta t^2} M + {}^{t+\Delta t}K^{(i-1)} \tag{18}$$

$$R_{eff} = {}^{t+\Delta t}R - {}^{t+\Delta t}F^{(i-1)} + M\left(\frac{9}{\Delta t^2}{}^{t+\Delta t}U^{(i-1)} - \frac{12}{\Delta t^2}{}^{t+\frac{\Delta t}{2}}U + \frac{3}{\Delta t^2}{}^{t}U - \frac{4}{\Delta t}{}^{t+\frac{\Delta t}{2}}\dot{U} + \frac{1}{\Delta t}{}^{t}\dot{U}\right) \tag{19}$$

The displacement increment at time $t+\Delta t$ can be calculated by substituting the

effective matrix obtained from equation 18 and 19 in equation 14 used in Newmark method. The final displacement is calculated by using the following equation.

$$^{t+\Delta t}U^{(i)} = {}^{t+\Delta t}U^{(i-1)} + \Delta U^{(i)} \tag{20}$$

Evaluating final velocity and acceleration in terms of displacement from equation 20, we have

$$^{t+\Delta t}\dot{U} = \frac{1}{\Delta t}\,{}^{t}U + \frac{4}{\Delta t}\,{}^{t+\frac{\Delta t}{2}}U + \frac{3}{\Delta t}\,{}^{t+\Delta t}U \tag{21}$$

$$^{t+\Delta t}\ddot{U} = \frac{1}{\Delta t}\,{}^{t}\dot{U} + \frac{4}{\Delta t}\,{}^{t+\frac{\Delta t}{2}}\dot{U} + \frac{3}{\Delta t}\,{}^{t+\Delta t}\dot{U} \tag{22}$$

Note that Newton-Raphson iterations are performed in equation 14.

For the dynamic analysis of jump ski model constructed by finite element method, the above time integration scheme was used at every time interval.

3.2.2 Contact & Friction method in FEM

There are various methodologies for including contact and friction conditions in FEM. Among them, friction condition can be implemented by using Lagrange multiplier method. The equilibrium and constraint equation including contact and friction force are as follow.[30]

$$MU + CU + KU = R - R_c(\mathrm{U}, \boldsymbol{\tau}) \tag{23}$$

$$F_c(\mathrm{U}, \lambda) = 0 \tag{24}$$

$$\boldsymbol{\tau} = [\lambda_1, \tau_1, ..., \lambda_k, \tau_k, ..., \lambda_m, \tau_m] \tag{25}$$

Where R_c is the nodal point force vector due to contact and friction, F_c is the constraint equation between two objects and bold $\boldsymbol{\tau}$ is the vector consisting of normal traction component and non-dimensional variable to obtain the tangential traction component.

In general, a coulomb friction model with a constant friction coefficient (μ_{dry}) is used for the simulation. If only the normal force is obtained from constraint equation about gap in the vertical direction, the frictional force can be calculated by the product of the constant coulomb friction coefficient and the normal force. Of course, constraint equation about friction is used in this case. But our friction model derived from theoretical model in icy condition is a function of pressure. When jump ski model comes in contact, contact length is calculated and substituted into the above equation 23,24 and 25 to obtain the frictional force. Thus, we need to know how to define the contact length. So, we performed the friction simulation

using the following friction model which is a function of pressure.

$$\mu = \frac{1}{P_r} = \frac{L_c}{F_n} \tag{26}$$

Frictional force has only one variable L_c. And our model is two dimensional. So, contact area A_c was replaced by contact length L_c.

$$F_f = L_c \tag{27}$$

Simulation tests were conducted using Euler beam elements with two and three nodes. The frictional force was analyzed by changing the length of the element.

As shown in the Figure 10, the beam element for the test is modeled as a simple straight line, and both contact and friction is generated at all the nodes. For an element with two nodes, the contact length is calculated by dividing each half of the element length (Figure 10(A)). In case of three nodes, it is divided into two elements based on the middle node, and the friction length at each node is calculated as the length corresponding to half of each element length. In particular, the middle node has the sum of the lengths corresponding to half of each element as the contact length (Figure 10(B)).

When the jump ski model constructed by finite element method moves with vibration, friction occurs, and then the friction model derived from parameter study is applied. The friction model is a function of pressure. Therefore, when the simulation is performed with vibration, contact length is calculated as above.

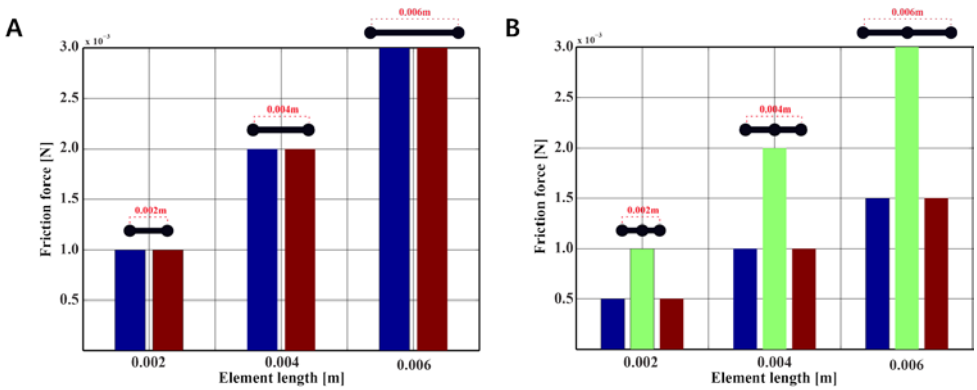

Figure 10. Simulation for analyzing how to contact lengths are calculated in FEM, (A) In the case of two nodes, contact length for each node is calculated as half the length of the element including the nodes where the contact occurred, (B) In the case of three nodes, the contact length is calculated in the same way as for the two nodes. But, the contact length is calculated as the sum of the half of each element length, especially at the middle node.

3.2.3 Simulation setup

Gravity acceleration was applied in the vertical direction and horizontal direction in consideration of the angle of in-run track. The constructed ski model pressed by vertical gravity comes in contact. After contact, the ski model began to move by the acceleration in the horizontal direction, and at this time, the tip and tail of the ski model were vibrated. As shown in Figure 11, the change of friction force is compared between when there was vibration and when there was no vibration. The influence of vibration was confirmed by changing the frequency of vibration from $50 rad/s$ to $200 rad/s$ when the amplitude of the vibration was constant at $25N$. It can be seen that the simulation results for the moving distance and terminal velocity without vibration are almost agreed with the results calculated by our assumption. It is also confirmed that the average frictional force is reduced by about 2% at vibration frequency $200 rad/s$, when compared to no vibration (Figure 11).

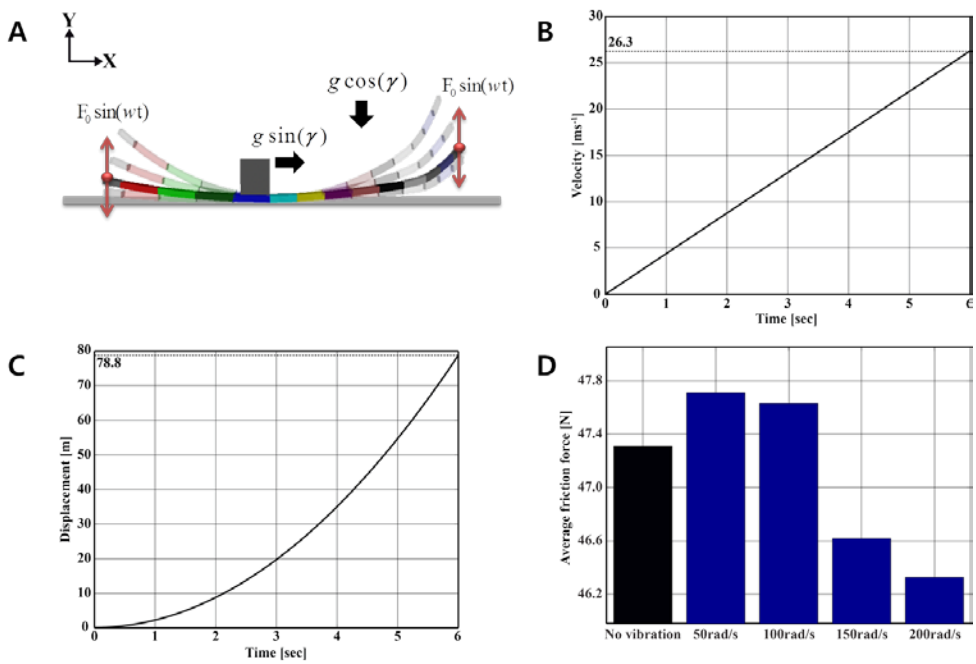

Figure 11. (A) Simulation setup. Gravity including angle of in-run track is applied in the each direction and vibration is applied to tip and tail of ski model, (B) Velocity obtained by simulation when there is no vibration, (C) Displacement obtained by simulation when there is no vibration, (D) Comparison between when vibration exists according to frequency and when there is no vibration.

3.2.4 Relationship between vibration mode and friction force

Jump ski has relatively long and slender geometry and consists of composite material. So, the elastic characteristics and configuration of ski itself can have an influence on friction when vibration is applied. As shown in Figure 11 (D), it can be seen that when the jump ski model is subjected to vibration, the average frictional force increases or decreases in a certain frequency range. This characteristic can be interpreted through the relationship between the friction model and the vibration mode of jump ski model.

Mode analysis is to find out the natural mode shapes and frequencies of object, which represent its own unique properties, and generalized equation of motion for analysis is

$$M\ddot{U} + KU = 0 \tag{28}$$

Where M is the mass matrix, K is the stiffness matrix, U is the displacement vector and an overdot is a time derivative.

To express the free vibration of an object rather than an external force, its displacement vector U is assumed to be harmonic motion as follow.

$$U = \Phi \sin(w_n t) \tag{29}$$

Where Φ is the eigenvector representing the displacement, w_n is the natural frequency and t is the time variable. Of course, the $\sin()$ function can be used as a $\cos()$ function. If the equation 29 is substituted for equation 28 with differentiated results, the equation 28 becomes

$$K\Phi = \lambda_n M\Phi \tag{30}$$

Where λ_n is the eigenvalue representing the square of natural frequency w_n.

In order to confirm the vibration characteristics of the jump ski model constructed by finite element method, the mode analysis was performed using the above method (Figure 12).

In the friction model obtained through the parameter study, 92.4% of the frictional force is caused by the hydrodynamic friction part and hydrodynamic friction is a function of the contact length as follows.

$$F_f = 0.0229F_n + 48.42L_c \tag{11}$$

Thus, if the shape of the vibration occurring at a specific frequency increases the average contact length of the ski during whole time, the average frictional force will increase and if it decreases, the average frictional force will decrease. The relationship between each mode and the frictional force was confirmed by substituting the corresponding mode frequency for the frequency of external vibration. It can be seen that the reduction rate of the average normal force and contact length is different for each frequency corresponding to modes. Particularly in the fourth mode, the greatest reduction of frictional force occurs (2.5%). Because the average normal force and the contact length decrease simultaneously by 2.5% (Figure 13).

The contact length and the normal force result for the entire analysis time are shown in Figure 14, which show that the contact length due to the vibration

become shorter from mode 1 to mode 6. However, the normal force is the smallest in the mode 4.

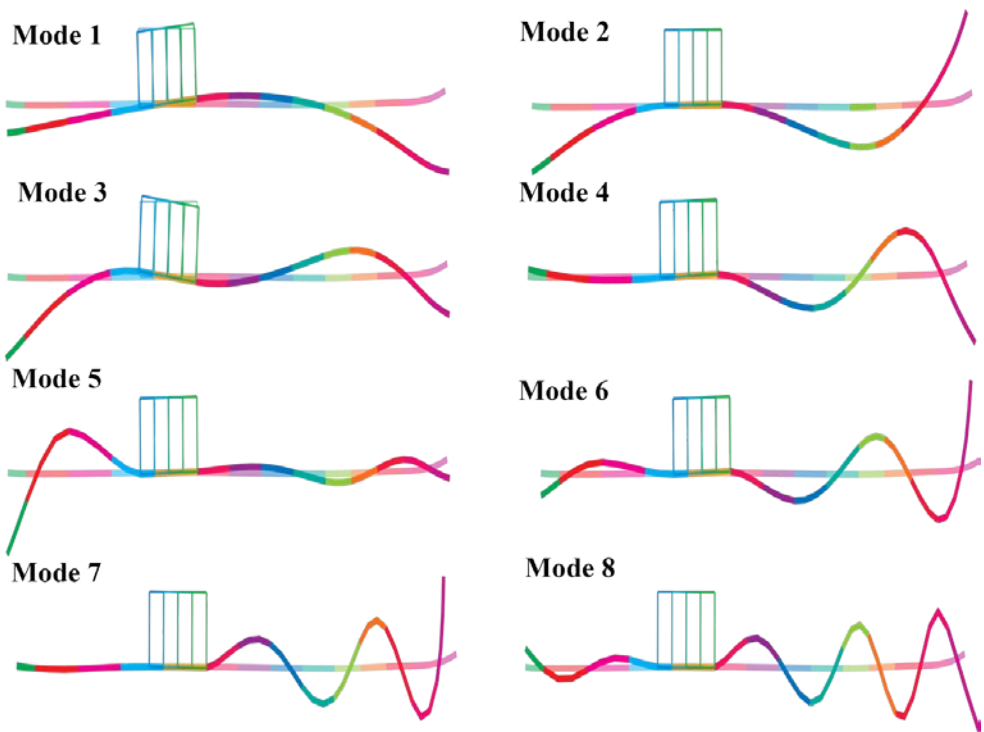

Figure 12. Mode shape for each mode. Natural frequency for each mode shape is in the Table 3.

Mode number	1	2	3	4	5	6	7	8
Frequency w_n [Hz]	9	23	30	59	101	107	173	259

Table 3. Mode analysis for jump ski model. These frequencies were used as the frequencies of external vibration.

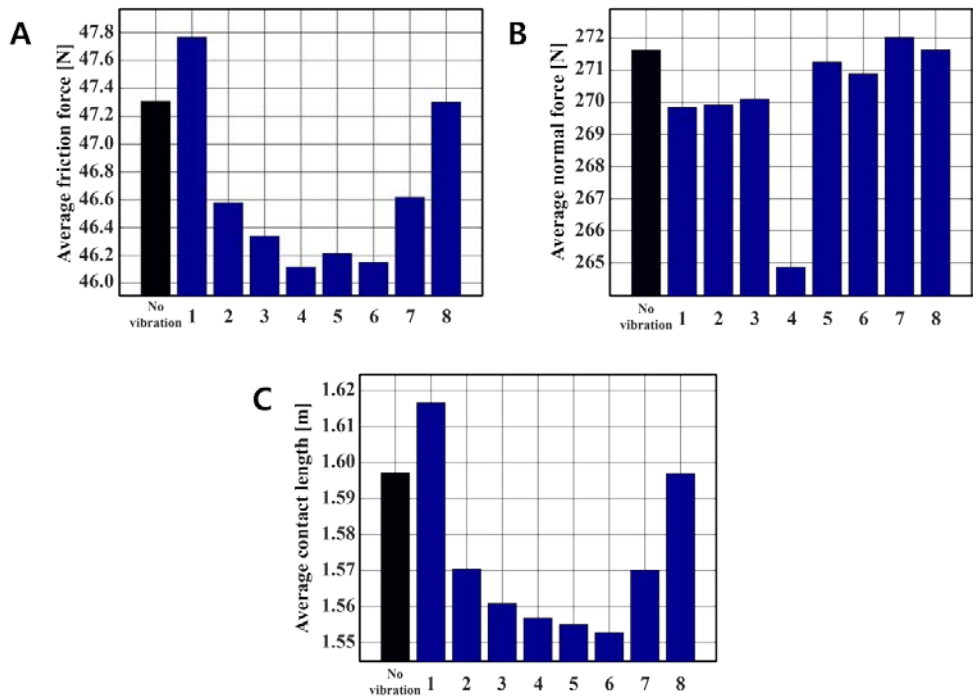

Figure 13. The relationship between vibration modes and friction, (A) Average friction force according to vibration mode. Mode number 4 has the smallest frictional force, (B) Average normal force. Mode number 4 has the smallest value, (C) Average contact length according to vibration mode. There is a specific frequency range that reduces the friction length.

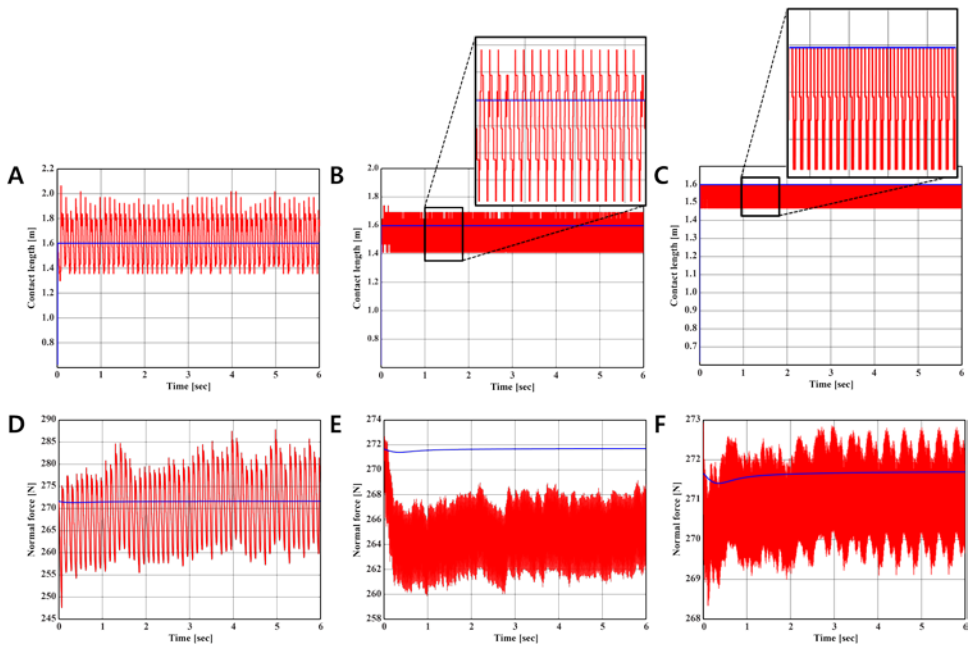

Figure 14. Contact length and normal force graph for mode 1, mode 4 and mode 6 as time goes on. Blue line indicates that there is no vibration, (A) Change in contact length at mode 1. The amount of increase in contact length by vibration is greater than the amount of reduction, (B) Change in contact length at mode 4. The amount of decrease in contact length by vibration is greater than the amount of increase, (C) Change in contact length at mode 6. The contact length only reduces by vibration. (D) (E) (F) Change in normal force at mode 1, 4, 6. At the mode 4 normal force is greatly reduced by the vibration.

4. Conclusion

As described in the introduction, a lot of researches have been done to reduce the frictional force through external vibration, but it has been limited to short and rigid test specimens that can’t show the elastic characteristics of the object. In essence, friction is heavily influenced by the environment in which the object is located, and it is very difficult to simulate the friction that occur every moment, especially since the friction occurs in icy condition through very complex process. Therefore, in order to analyze the physical phenomenon occurring in the in-run state of ski jump, we constructed a finite element model which can show the elastic characteristics of real jump ski and confirmed that the elastic characteristics of the constructed jump ski model fit well with experimental results. Next, based on the experimental data of friction in icy condition using the base material of ski, the friction model was derived by performing the parameter study on the theoretical friction model. Finally, the effect of the vibration generated during skiing on the friction force was simulated and obtained results that the average friction force decreased or increased at a specific frequency of vibration. Further, in order to analyze the correlation between the external vibration and the friction, we investigated the relationship between vibration modes of the jump ski model and the induced friction model.

In an induced friction model, most of the frictional force is generated by the hydrodynamic friction part, and that frictional force is a function of contact length. Therefore, it is possible to find the cause of the decrease or the increase of the frictional force at a specific frequency through the relation between the elastic characteristics of the ski model and the contact length.

References

1. M, LEUS., P, GUTOWSKI. (2008) Analysis of longitudinal tangential contact vibration effect on friction force using coulomb and dahl models, Journal of Theoretical and Applied Mechanics, 46, 1, pp.171-184.

2. M, Sfakiotakis., N, Pateromichelakis., D, P. Tsakiris. (2014) Vibration-Induced frictional reduction in miniature intracorporeal robots, IEEE Transactions on Robotics, Vol 30, No. 5.

3. A. LEHTOVAARA. (1987) INFLUENCE OF VIBRATION ON THE KINETIC FRICTION BETWEEN PLASTICS ANS ICE, Wear, Vol 115, pp.131-138.

4. P. OKSANEN., J. Keinonen. (1982) THE MECHANISM OF FRICTION OF ICE, Wear, Vol.78, Issue 3, pp.315-324.

5. L. Bäurle., D. Szabó., M. Fauve., H. Rhyner., N. D. Spencer. (2006) Sliding friction of polyethylene on ice:tribometer measurements, Tribology Letters, Vol. 24, No. 1, pp.77-84.

6. L. Bäurle., U. Kaempfer., D. Szab ó., N.D. Spencer. (2007) Sliding friction of polyethylene on snow and ice: Contact area and modeling, Cold Regions Science and Technology, Vol. 47, Issue 3, pp.276-289.

7. Lasse Makkonen., Maria Tikanmäki. (2014) Modeling the friction of ice, Cold Regions Science and Technology, Vol. 102, pp.84-93.

8. Robert Kostek. (2009) INFLUENCE OF AN EZTERNAL NORMAL HARMONIC FORCE ON REDUCTION OF FRICTION FORCE, Journal of POLISH CIMAC 4, pp.67-73.

9. Akira Shionoya., Toshio Kobayashi., Toshinori Saijo., Kenichiro ogata., Toshiaki Matsuhashi. (2008) Flexural vibration of jump Ski in Flight, Bio-mechanism of Swimming and Flying, Springer japan, pp.383-394.

10. Anne-Marie Kietzig., Savvas G. Hatzikiriakos., Peter Englezos. (2010) physics of ice friction, Journal of Applied Physics, Vol. 107, Issue 8.

11. J.T. ODEN., J.A.C. MARTINS., (1985) Computer Methods in Applied Mechanics and Engineering, Vol. 52, Issue 1-3, pp.527-634.

12. K. J. Bathe., Anil B. Chaudhary. (1985) A solution method for planar and axisymmetric contact problems, International Journal for Numerical Methods in Engineering, Vol. 21, Issue 1, pp.65-88.

13. Anil B. Chaudhary., K. J. Bathe. (1986) A solution method for static and dynamic analysis of three-dimensional contact problems with friction, Computer & Structures, Vol. 24, Issue 6, pp.855-873.

14. K. J. Bathe., P. A. Bouzinov. (1997) On the constraint function method for contact problems, Computer & Structures, Vol. 64, Issue 5-6, pp.1069-1085.

15. A. L. Eterovic., K. J. Bathe. (1991) On the treatment of inequality constraints arising from contact conditions in finite element analysis, Computer & Structures, Vol. 40, Issue 2, PP.203-209.

16. Daniel Pantuso., K. J. bathe., Pavel A. Bouzinov. (2000) A finite element procedure for the analysis of thermos-mechanical solids in contact, Computer & Structures, Vol. 75, Issue 6, pp.551-573.

17. MA Chowdhury., MM Helali. (2008) The effect of amplitude of vibration on the coefficient of friction for different materials, Tribology International, Vol. 41, Issue 4, pp.307-314.

18. MA Chowdhury., MM Helali. (2006) The effect of frequency of vibration and humidity on the coefficient of friction, Tribology International, Vol. 39, Issue 9, pp.958-962.

19. Takeshi Yoneyama., Motoki kitade., kazutaka Osada. (2010) Investigation on the ski-snow interaction in a carved turn based on the actual measurement, Procedia Engineering, Vol. 2, Issue 2, pp.2901-2906.

20. Peter Federolf., markus Roos., Anton Lüthi., Jürg Dual. (2010) Finite element simulation of the ski-snow interaction of an alpine ski in a carved turn, Sports Engineering, Vol. 12, Issue 3, pp.123-133.

21. W. Littmann, H. Storck, J. Wallaschek. (2001) Sliding friction in the presence of ultrasonic oscillations: superposition of longitudinal oscillations, Archive of Applied Mechanics, Vol. 71, Issue 8, pp.549-554.

22. VC Kumer., IM Hutchings. (2004) Reduction of the sliding friction of metals by the application of longitudinal or transverse ultrasonic vibration, Tribology International, Vol. 37, Issue 10, pp.833-840.

23. Maiko Takeda., Kunio Nikki., Takaaki Nishizuka., Osamu Abe. (2010) Friction of the short model at low velocity, Journal of Physics: Conference Series, Vol. 258, No. 1.

24. K. Schindelwig., M. Hasler., J. Van Putten., S. Rohm., W. Nachbauer. (2014) Temperature Below a Gliding Cross Country Ski, Procedia Engineering, Vol. 72, pp.380-385.

25. SC Colbeck, L Najarian., (1997) HB Smith. Sliding temperatures of ice skates, American Journal of Physics, Vol. 65, Issue 6.

26. F. P. Bowden., T. P. Hughes. (1939) The mechanism of sliding on ice and snow, Proceedings of the Royal Society of London. Mathematical & Physical Sciences, Vol. 172, Issue 949, pp.280-298.

27. D. C. B. Evans., J. F. Nye., K. J. Cheeseman. (1976) The Kinetic Friction of Ice, Proceedings of the Royal Society of London. Mathematical & Physical Sciences, Vol. 347, No. 1651, pp.493-512.

28. K. J. Bathe., Mirza M. Irfan Baig. (2005) On a composite implicit time integration procedure for nonlinear dynamics, Computers & Structures, Vol. 83, issues 31-32, pp.2513-2524.

29. F. P. Bowden. (1953) Friction on Snow and Ice, Pro. Roy. Soc., A, Vol. 217,

Issue 1131, pp.462-478.

30. K. J. Bathe. (2015) Finite element procedure, pp.622-627.

Abstract (Korean)

얼음에서 마찰은 boundary, mixed 그리고 hydrodynamic 영역으로 구성된 매우 복잡한 현상이다. 물체와 얼음 사이에서 생성된 물 층의 두께, 마찰에 의한 열, 물체의 속도 및 마찰 면적과 같이 다양한 요소들이 이 영역들에서 발생하는 마찰에 영향을 준다. 스키점프에서 스키가 얼음으로 만들어진 경기장을 활강할 때 많은 진동이 발생하며 그 진동은 위에서 언급한 여러 요소들에 영향을 미칠 수 있다. 여기서 우리는 얼음에서 마찰이 발생할 때 일반적으로 적용되는 이론적인 마찰모델을 이용하여 수치적으로 진동이 마찰에 미치는 영향을 살펴보았다. 먼저 스키 바닥재료와 얼음 사이의 마찰 실험을 통해 얻어진 데이터를 이용하여 이론적 마찰모델에 대한 파라미터 연구를 진행하였으며 압력을 변수로 하는 마찰모델을 유도하였다. 그리고, 탄성특성이 실험과 잘 맞는 점프 스키 모델을 유한요소를 이용하여 구축하였다. 마지막으로 시뮬레이션을 통해 어떻게 진동이 마찰에 영향을 주는지 살펴보았다.